

General Disclaimer

One or more of the Following Statements may affect this Document

- This document has been reproduced from the best copy furnished by the organizational source. It is being released in the interest of making available as much information as possible.
- This document may contain data, which exceeds the sheet parameters. It was furnished in this condition by the organizational source and is the best copy available.
- This document may contain tone-on-tone or color graphs, charts and/or pictures, which have been reproduced in black and white.
- This document is paginated as submitted by the original source.
- Portions of this document are not fully legible due to the historical nature of some of the material. However, it is the best reproduction available from the original submission.

**NASA TECHNICAL
MEMORANDUM**

NASA TM X-73522

NASA TM X-73522

(NASA-TM-X-73522) THERMAL-ENVIRONMENT
TESTING OF A 30-cm ENGINEERING MODEL
THRUSTER (NASA) 23 p HC A02/MF A01 CSCL 21C

N77-12121

Unclas
G3/20 54564

**THERMAL-ENVIRONMENT TESTING OF A 30-CM
ENGINEERING MODEL THRUSTER**

by Michael J. Mirtich
Lewis Research Center
Cleveland, Ohio 44135



**TECHNICAL PAPER to be presented at the
Twelfth International Electric Propulsion Conference sponsored by the
American Institute of Aeronautics and Astronautics
Key Biscayne, Florida, November 15-17, 1976**

Thermal-Environment Testing of a 30-cm Engineering Model Thruster

Michael J. Mirtich
National Aeronautics and Space Administration
Lewis Research Center
Cleveland, Ohio 44135

Abstract

An experimental test program was carried out to document all 30-cm electron bombardment Hg ion bombardment thruster functions and characteristics over the thermal environment of several proposed missions. An engineering model thruster was placed in a thermal test facility equipped with -196°C walls and solar simulation. The thruster was cold soaked and exposed to simulated eclipses lasting in duration from 17 to 72 minutes. The thruster was operated at quarter, to full beam power in various thermal configurations which simulated multiple thruster operation, and was also exposed to 1 and 2 suns solar simulation. Thruster control characteristics and constraints; performance, including thrust magnitude and direction; and structural integrity were evaluated over the range of thermal environments tested.

I. Introduction

As part of the solar electric propulsion (SEP) technology readiness program at Lewis, an experimental test program was performed to demonstrate 30-cm Hg-ion bombardment thruster functions over the thermal environment of various proposed missions.^{1,2,3} Goals of the program were to: (1) demonstrate mechanical integrity of the Engineering Model thruster stored at background temperatures as low as LN_2 (-196°C), (2) verify that neither temporal nor spatial thermal gradients had adverse effects on thruster components or thruster operation, (3) verify that the thruster could operate at quarter-, half-, and full-beam power when exposed to on-axis solar simulation from zero to 2 suns, (4) verify that other thrusters, operating in close proximity, do not present thermal problems, and (5) define thruster restart characteristics with a variety of simulated eclipse conditions. Another goal of the program was to characterize the thruster as a thermal element in the total spacecraft system and generate sufficient data for the development of a thermal model of the thruster.

II. Apparatus

Facility

To implement this program a facility capable of providing thruster background temperatures of liquid nitrogen (-196°C) was developed. This was accomplished by modifying a 1.5-meter diameter by 5.1-meter long vacuum tank equipped with four oil-diffusion pumps. This modified tank, along with the position of the thruster in the tank, is sketched in Figure 1. This tank had a cylindrical liquid nitrogen (LN_2) baffle that was only 4.5-meter long and radiation shielding, consisting of aluminum and aluminized Mylar, was attached to the ends of the LN_2 baffle to reduce the thermal loading from the room temperature tank walls (see Fig. 1). The aluminum shielding was spray painted with a layer of graphite to reduce sputtering and provide a better background for solar illumination by reducing reflections. Aluminum and aluminized-Mylar shielding were also placed between the diffusion pumps on

the floor of the tank and in places where gaps occurred in the LN_2 baffle. These facility modifications provided uniform background temperatures. Except for the radiation shields at the ends of the baffle, these temperatures remained nearly constant during thruster operation. Temperatures at the upstream radiation shield (behind the thruster) increased due to thermal loading from the operating thruster. The downstream (target) shield increased in temperature from the bombardment of the Hg-ion beam. The target radiation shield had a hole 30 cm in diameter on the tank centerline to allow on-axis solar illumination of the thruster. A quartz window 26 cm in diameter was located on the centerline of the tank end flange. This window was protected with a movable shield when not in use.

Thruster

The thruster, was the modified 700 series (702-A) shown in Figure 2 and had grids with a 1.25 cm dish. (The accelerator and screen grids were 43 and 67 percent open, respectively.) This thruster, unlike the 400 series thruster thermally tested in reference 4, had a split cathode-isolator vaporizer system.⁵

Some materials used in the 702-A thruster were different from those in the 400 series thruster previously tested. On the 702-A thruster the anode was made of Ti, the backplate Ti, the outer shell Ti, and the rear cover Al. On the 400 series these thruster components were made of stainless steel. A difference between the 702-A thruster and the engineering model 900 series thruster is the baffle-pole piece assembly and the screened backplate-anode.⁶ However, because of similarity in construction and design, no significant thermal difference exist between the 702-A thruster and the 900 series EMT.

Thruster mount system and thermocouple locations. The thruster was supported by four ceramic (Al_2O_3) rods 5-cm in diameter by 5-cm long. The ceramic supports served the dual purpose of providing both electrical and partial thermal isolation for the thruster. The ceramic was in turn attached to an aluminum collar to give structural support. This thruster assembly was then attached to an end flange by four, 2.54-cm diameter, 183-cm long aluminum rods. The aluminum rods allowed the thruster to extend through the radiation shield and into the tank. Figure 3 is a back view of the thruster and its mount system.

All power leads, propellant feed lines, and thermocouple leads came out the back of the thruster and were contained inside the aluminum-rod-mount system. This allowed control of any conduction losses incurred by these leads or feed lines. These losses were calculated to be about 80 mW for all thermocouples, 190 mW for the feed lines, 44 mW for the Hg in the feed lines and 2.2 W for the supports, and are insignificant w.r.t. the total power dissipated in the thruster discharge.

The thruster, the mercury feed lines, and thruster mount system were instrumented with 40 Chromel-Alumel (C-A) thermocouples. The 26 thermocouples located in the thruster are shown in Figure 4 and are listed in table II.

Solar Simulation

Shown in Figure 5 is the 40 kW carbon arc lamp used for solar simulation. The lamp radiation was collected through a movable quartz lens system to allow either one or two suns intensity (0.7 A.U.). In reference 7 it was shown that the carbon arc spectrally matched the Johnson curve for the solar spectrum very closely. The solar intensity was obtained by measuring the short circuit current of a N/P silicon solar cell along with a calibrated, water cooled, radiometer.

The solar beam flux density was uniform to within 5 percent at the grid plane of the thruster. The diameter of the solar beam at that plane was over 60 cm which was sufficient to cover the thruster and azimuthal heat shield surrounding the thruster. Over the time periods run in these experiments, sometimes greater than 5 hours, there was little or no variation in intensity of the solar simulation. Also from run to run the same conditions could be duplicated. Thus, no appreciable changes occurred in the performance of the entire solar simulation system over the test period.

Thruster Thermal Environment

Four thruster thermal environments were selected for thermal testings to provide sufficient data for development of an analytic model of the thruster. Thermal configuration I (Fig. 6) had no radiation shielding surrounding the thruster so that thruster surfaces radiated directly to the surrounding cold tank walls, except for the rear which saw a heat shield 7.6-cm behind the thruster. (The rear shield was made of aluminum and had C-A thermocouples to indicate shield temperature.) This thermal configuration allowed a maximum interaction with a space environment and a minimum thermal interaction with other thrusters. This configuration would be expected to achieve the coldest thruster temperatures in either operated or stored modes in a simulated space environment and most closely represents the thermal conditions for a deep space mission. Configuration I was also used to establish the measured bounds of the thruster during eclipse simulations.

Configuration II (Fig. 6) had a 360° azimuthal shield around the thruster. This shield had heaters so that the temperature of the shield could be controlled to simulate the thermal input of other thrusters. The rear shield 30 cm by 30 cm was located 30 cm behind the thruster giving the rear of the thruster a view factor to LN₂ walls of 0.70. This configuration (II) was used to assess the impact of other operating thrusters surrounding the thruster and also provided uniform azimuthal background temperatures for correlation data to generate an analytic thermal model.

Thermal configuration III (Fig. 6) was similar to configuration II except that an additional shield of aluminized mylar (Al/mylar) was placed between the thruster and the azimuthal shield as well as the rear shield to reduce to a negligible value all the heat rejection to the rearward hemisphere. This

configuration (III) simulated a condition of a thruster thermally isolated from the spacecraft and other thrusters. The aluminized-Mylar heat shielding was made of 0.0012 cm thick Mylar, coated on both sides with 1000 Å aluminum. The aluminized-Mylar radiation shields used between the azimuthal and rear shield consisted of six concentric cylinders. In addition this configuration was used to simulate a multiple thruster environment.

Thermal configuration IV was identical to configuration III except that the 360° azimuthal heat shield had a 90° segment removed in the upper quadrant. This was done in an attempt to simulate asymmetric thermal loading of the thruster.

III. Cold Storage and Start Up

Many missions^{1,2,3} require long term storage of a thruster and also restarts over a large range of thermal environments. During storage, the thruster can become very cold, such that mercury could be frozen in the feed lines. Tests were run to simulate conditions where the mercury in the feed lines were frozen in order to determine that during exposure to the cold environment of space the structural integrity of the thruster would be maintained.

The thruster was cold soaked in the laboratory about 20 times with various thermal configurations and the coldest temperatures attained are shown in Figure 7 (configuration 1). The coldest thruster temperatures attained in this configuration were -92° C on the engine body and the anode. The cold soak equilibrium temperatures were reached in about 24 hours. No structural changes were ever observed in the thruster as a result of the cold soak tests.

A number of startup tests were carried out to verify mechanical integrity and characterize system requirements to achieve startup. The startup from these conditions was expected to bound the system startup requirements for thruster storage at large A.U. missions. Normal startup⁸ from frozen conditions was attempted using configuration I, where the coldest thruster temperatures were attained. Generally, for all the tests the initial temperature conditions of the thruster were the same, and mercury was frozen in the feed lines. The distance upstream of the vaporizers that the mercury was frozen depended on the thermal configuration, and will be presented later.

With the thruster extended into the tank as shown in Figure 1, 152 cm of the Hg neutralizer, cathode and main propellant lines were exposed to LN₂ walls of the tank. In the preheat mode, 60 watts was applied to the neutralizer tip heaters, 60 watts to the cathode tip heater, and 45 watts to the cathode and main isolators. The thermal feed back from the tip heaters and isolators caused a rapid rise in temperatures at the vaporizers, such that after 20 minutes the main vaporizer temperature was 124° C, the cathode vaporizer temperature 98° C and the neutralizer temperature 80° C. At 20 minutes the vaporizers were turned on to full power, and the isolator power turned off. The cathode and neutralizer lit indicating no structural changes in these cathodes and at t = 38 minutes, the maximum beam attained was 0.75 amps. However, because of the length of frozen feed line the thermal feed back from the discharge was insufficient to thaw the feed lines. As a consequence,

liquid Hg could not be supplied and a discharge could not be sustained. Within minutes, due to the lack of a Hg pressure head on the vaporizer plug, the cathodes went out.

With the thruster in thermal configuration I, other attempts were made to thaw the feed lines and start up the thruster using power applied to thruster components only. These attempts included adding various combinations of tip heater power and vaporizer power for periods of time up to 20 hours. Thermocouples placed on the feed lines at various locations upstream of the thruster are sketched in Figure 8 along with temperature levels (open symbols) at these locations at $t = 0$ (frozen) before any power was applied to the heaters or vaporizers. With 10 watts to each isolator and 4 watts to each vaporizer, the temperature levels after 20 hours (solid symbols) are indicated for each vaporizer and some locations on its feed line system right up to the Hg reservoir outside the tank. As shown in the figure the thermocouples located 145 cm from the thruster back plate did not change temperature and hence, were not significantly affected by the thruster thermal feed back. The temperature levels of the feed lines were near the temperature level of frozen Hg at distances from the thruster back plate of 38 cm for the neutralizer feed line, 51 cm for the main vaporizer feed line and 63 cm for the cathode feed line thruster. At startup, temperatures indicated that Hg was still frozen in the feed lines. The addition of 1 sun simulated solar input to the thruster front was not enough input energy to thaw the feed lines. However, it should be noted that no structural problems occurred because of these conditions.

To show that it was possible to start and sustain a discharge in the 702 thruster with Hg frozen in the feed lines, a 91 cm diameter bell jar was added to one end of the tank to reduce the length of feed line exposed to LN_2 . In this configuration (tank, bell jar, and thermal configuration I) the thruster was cold soaked until frozen in the lines to at least the tee couplings. A conventional startup using cathode tip and isolator power was then performed. In addition small amounts of power were applied to the vaporizers in order to help thaw the frozen mercury. Three watts of power was used at the cathode and main vaporizers and 10 watts at the neutralizer vaporizers (since the neutralizer is isolated from the rest of the system more power was used). From this frozen condition it was possible to attain at full beam of $J_B = 2A$ in 34 minutes with a minimum of breakdown.

Absolute techniques in starting from a frozen thruster condition to match any of the multiple missions that may exist for an EM thruster and its power processor were not within the scope of these experiments. A goal here was to establish that it is possible to attain full beam power, in the EM thruster from a frozen condition, without any structural problems occurring in the thruster.

The results of starting a thruster from cold storage are: (1) there is no mechanical or structural damage to the thruster during this time of maximum thermal stress with or without Hg frozen in the feed lines, (2) with Hg frozen at least 38 cm from the thruster vaporizers, a conventional restart, with some power applied to the vaporizers, was insufficient to sustain a discharge, and (3) with Hg frozen in the feed lines only near the

thruster it was possible to attain a full beam of 2 amperes in 34 minutes with a conventional restart plus the addition of vaporizer heater power.

IV. Eclipse Simulation

In some proposed near earth missions the spacecraft-thruster system will experience eclipses for up to 72 minutes. For such missions it is desirable to return to the thruster pre-eclipse power condition in as short a time as possible. Tests were performed to simulate eclipse conditions over a number of thruster operating and environmental conditions. The procedure followed was to let the thruster approach thermal equilibrium at a given beam power and solar simulation condition. The sun simulator (if used) and all power to the thruster were then turned off and the temperatures on the thruster recorded. Although a range of eclipse conditions were simulated only the ones which are important to envelope the thruster thermal constraints will be presented here.

One eclipse condition is a thruster operating at low beam power and a short duration eclipse. The first thruster (configuration I) exposed to an eclipse was running at low beam, $J_B = 1A$. Shown in Figure 9 are the temperature-time profiles of the vaporizers during a 17-minute simulated eclipse and the corresponding rises in vaporizer temperature during restart to a 1 amp beam 16 minutes after the thruster came out of the eclipse. A conventional restart was attempted but due to the warm nature of the thruster this technique did not result in a successful restart. Several tests were performed to define a restart technique that would assure success in this short eclipse condition. The following startup sequence was found to be successful: Sixty watts was applied to the cathode and neutralizer tip heaters, and no power was applied to the isolator. The cathode and main vaporizers are still warm at $t = 17$ minutes and isolator power can vaporize Hg and cause an undesirable cathode ignition or Hg condensation in the discharge chamber. After heating the cathodes for 10 minutes ($t = 27$ min), the vaporizers for the cathodes were placed on controllers, the keeper supplies were turned on and the main vaporizer set to 3 watts. The main vaporizer was not placed in controllers, since with no beam the controller would call for full vaporizer power and the excessive Hg vapor can cause breakdowns when the high voltage is turned on. One minute after the vaporizers were turned on, the neutralizer lit ($t = 28$ min). The cathode lit and discharge was established at $t = 30$ minutes, or 13 minutes after the end of the eclipse. The high voltage was also turned on at $t = 30$ minutes and 16 minutes after the eclipse ($t = 33$ min) the thruster was back to the pre-eclipse value of beam current at a 1 amp beam.

The longest expected eclipse in near earth orbit is one of 72 minutes. Figures 10(a) and (b) show cool-down curves for the vaporizer and other thruster components for thermal configuration I for a 72 minute eclipse. The open symbols are for a thruster operating at full beam power exposed to 1 sun before the start of the eclipse and the closed symbols represent the cooling curves of the same thruster with no sun before the start of the eclipse. Figure 10 shows the initial temperature values of various thruster components for the variable sun simulation. It is seen that after the eclipse simulation the components cooled at different rates up to about 30 minutes. After 30 minutes

each component temperature was nearly independent of its initial temperature value. This means, that for eclipse simulation of greater than 30 minutes, sun simulation prior to the eclipse is not necessary to obtain cooling curves of thruster components. A point also clear in Figure 10(a) is that vaporizer cooling is not strongly affected during an eclipse by the temperature levels of other thruster components.

After the thruster had been in the eclipse mode for 72 minutes, a conventional restart was initiated and the Engineering Model thruster attained a full beam in 15 minutes.

These studies indicate that little or no thermal problems arise during an eclipse w.r.t. the thruster. However, the duration of the eclipse can significantly affect the restart sequencing of the thruster to either a one or two amp beam current. The restart of the thruster after an eclipse was done with laboratory power supplies designed at Lewis and restart capability compatible with the entire spacecraft system (solar cell array, and space power processor) is yet to be demonstrated.

V. Solar-Multiple Thruster Simulation Thermal

Equilibrium Tests

Operating Procedure

The object of these tests was to operate a 30-cm thruster at quarter, half, and full beam power and determine the effects of thermal environments on the closed loop control of the thruster, the thrust vector, and accelerator grid system integrity. To accomplish this objective, a number of tests with the four thermal configurations were performed.

The steady state control of a thruster is achieved by means of set point parameters and via proportional control of three vaporizers which are used to hold three thruster parameters constant. The beam current, discharge voltage and neutralizer keeper voltage are held at constant values by proportional control of the heater power to the main, cathode and neutralizer vaporizers, respectively. Accommodation of changes in the thermal environment can be accomplished by adjusting the power settings to the vaporizers. If the thermal input from the environment and thruster decrease the vaporizer heater power to zero, control is lost. Tests were run over a large range of conditions to determine the margin for proportional control. Proportional controllers similar to those of reference 9 were used for all tests. Power settings of the vaporizers for each of the environmental test conditions are shown in table 1.

The thrust vector was measured with a molybdenum probe 1.25 cm in diameter and 1.0 m downstream of the measured beam profile at each test condition.

Accelerator grid integrity was evaluated by measuring the permeance and the high voltage breakdown rates. Variations of either would indicate grid movement or other phenomena which could impact the operation of the grid system.

For each thruster power setting the thruster was exposed to 0, 1, or 2 suns on axis solar simu-

lation. The data taken once thermal equilibrium was reached also included the temperatures of thruster components as a function of discharge power and solar flux (table II). To attain thermal data the thruster was first allowed to come to thermal equilibrium, which usually took 4 to 5 hours, with no solar illumination. The solar simulator was then turned on. After about 2.5 hours of solar illumination, the thruster again attained thermal equilibrium. Presented in the next sections are some of the data taken for each thermal configuration.

Thermal Configuration I

In thermal configuration I some of the thruster surfaces radiated directly to the cold tank walls. The rear of the thruster, however, had a view factor of about 0.7 to the rear shield whose temperature was around 40° C, to simulate a spacecraft surface. The thruster conditions run for this thermal configuration were beam currents (J_B) of 1/2, 1, and 2 amps.

Presented in table II and also shown in Figure 11 are the temperature levels of various thruster components as a function of discharge power for 0 and 2 sun illumination for thermal configuration I. The zero sun case represents a mission of large A.U. from the sun where the thermal input from the sun and other thrusters is negligible. No thruster operating problems were experienced, for this thermal condition, even at the lowest beam current level (quarter power), where the lowest equilibrium operating temperatures were reached (0° C on the ground screen). From the figure, it can be seen that increasing the discharge power increases the temperature levels of most of the components shown. It should be noted that as the discharge power increases the cathode vaporizer and main vaporizer temperatures are controlled by proportional controllers to provide the Hg flows needed to attain proper performance. A large thermal gradient exists between the front and back of the anode because most discharge electron are collected near the front end.¹⁰ At 375 watts discharge power ($J_B = 2$ amps) a temperature difference of 160° exists. The dashed curves show the increase in temperature levels for the various components during exposure to 2 suns. The largest increases in temperature take place at the lowest power levels, due to the relative energies of the sun output and thruster power levels.

Shown in Figure 12 and table I are the power settings needed to keep the temperatures at the vaporizers constant at full beam power ($J_B = 2A$), as a function of solar illumination. These reductions occur due to rises in temperatures of thruster components from solar radiation and the associated thermal feedback to the vaporizers. Though the vaporizer power settings are reduced as the solar flux is increased there is no loss of control for this baseline case (thermal configuration 1). The margin for control will, of course, depend somewhat on the characteristic of the vaporizer itself. The vaporizers used on the 702-A thruster operate at full beam power at temperature levels of 311° C for the main vaporizer, 282° C for the cathode vaporizer, and 277° C for the neutralizer vaporizer. The temperature level of the cathode vaporizer was somewhat lower (~20° C) than that for the present EMT design.¹¹ Figure 12 indicates that the maximum tolerable solar flux will be determined by the

cathode vaporizer control margin and is estimated to be approximately 4 suns.

Shown in Figure 13 is a plot of the ratio of the drain current to the beam current (J_A/J_B) versus the total accelerating voltage for beam currents of 1 and 2 amps, without and with 1 and 2 suns solar illumination. Also shown are the temperature levels of the edge of the accelerator grid for these conditions. This data indicates no change in perveance for the baseline case due to solar heating of the accelerator grid; i.e., no change in grid spacing. Thruster performance data also taken indicate no change in grid spacing.

Changes in grid gap can also cause changes in beam profile. Shown in Figure 14 is a typical plot of part of the beam profile as measured by the moly button probe at full beam power for 0, 1, and 2 suns. The probe could cover only a little over half the beam. No change in beam profile was detected at this thermal configuration or any of the other thermal configurations tested.

The thruster in this configuration was also run at $J_E = 10.6$ A, $\Delta V_I = 35$ V, and $J_B = 2$ A with little or no differences in temperature levels or power settings from the thruster run at $J_E = 10$ A, $\Delta V_I = 37$ V, and $J_B = 2$ A.

Thermal Configuration II

Shown in Figure 15 are the temperature levels of various thruster components as a function of discharge power for thermal configuration II with no sun (the temperatures of all the components measured are presented in table II). For the data plotted in this figure the azimuthal shield temperature at each power setting was equal to the average of the engine body and ground screen temperature. However, for zero power input to the shield its equilibrium temperature was 90° C at $J_B = 2$ A and zero sun. Comparison of temperature levels of specific components for configuration II with the temperature levels of the same component for configuration I of Figure 11, show that there is an increase in temperature of all the components presented for each discharge power. For example, at a 2 amp beam current the anode front temperature level increased to 450° C from 401° C in thermal configuration I. Even though some temperatures, like the manifold and back of the anode were close to cathode vaporization temperatures, no loss of control of the thruster occurred.

Shown in Figure 16 is the effect of the azimuthal shield temperatures on thruster temperature levels for a thruster operating at full beam power and 0 sun. The shield temperature was varied from 90° C (0 power to shield) to 250° C. Also shown are the temperatures of the thruster components with no shield, the thruster having a view factor to LN_2 . Some components like the front of the anode and the cathode flange show little or no increase in temperature as the azimuthal shield temperature is increased. The thruster component most affected by shield temperature changes is the ground screen which rises in temperature from 140° C at a shield temperature of 90° C to 220° C at a shield temperature of 250° C. This rise in ground screen temperature transfers to other components, i.e., an increase in the engine body temperature.

Associated with the rise in azimuthal shield

temperatures, there were some decreases in power settings to the main and cathode vaporizers. At a shield temperature of 90° C, the main vaporizer power setting was 6.2 watts, the cathode vaporizer 3.3 watts, and the neutralizer 4.1 watts. At a shield temperature of 250° C, the power settings were reduced to 85, 58, and 90 percent of their initial values for the main, cathode, and neutralizer vaporizers, respectively. Shown in Figure 17 is a plot of the power required for the main, cathode, and neutralizer vaporizer for $J_B = 2$ A (full beam power) as a function of on axis solar illumination of 0, 1, and 2 suns for thermal configuration 2. For the power shown at 0 suns the azimuthal shield temperature was 220° C and at 2 suns the shield temperature was 250° C. There are reductions in power with solar intensity and for all the vaporizers, but all reductions were well within the thermal control margin of the vaporizers. Thus, even with the thruster surrounded with an azimuthal temperature of 250° C and 2 suns illumination, there was no loss of control of the thruster.

For all the above conditions for configuration II there was no change in beam profile, hence, no change in thrust vector. In addition, there was no change in either the perveance or an increase in the high voltage breakdown rate due to multiple sun illumination. Hence, there was no change in thruster performance as a function of solar illumination or thermal configuration.

Thermal Configuration III

For thermal configuration III, six wraps of aluminized Mylar was placed between the azimuthal shield and the rear heat shield to negate any view factor of the thruster rear or sides to LN_2 walls. This is an extreme experimental thermal configuration of multiple thruster operation, for a thruster never has such a high view factor (nearly 100 percent) of other operating thrusters. However, exposing a thruster exclusively to warm background temperatures allows one to find the temperature levels that do effect thruster performance, and can represent test cases where the thruster is thermally isolated from other thrusters and from the rearward hemisphere.

Shown in Figure 18 are the temperature levels of various thruster components as a function of discharge power for thermal configuration III with no sun. The 360° azimuthal shield temperature is also plotted, and was the average of the ground screen and engine body temperatures for each discharge power level. When compared to the temperature levels of configuration II (Fig. 15), the largest increase in temperature is for the rear cover, which rose to 200° C from 175° C in configuration II. At the temperature levels shown in Figure 18, there was no loss of control of the vaporizers.

Plotted in Figure 19 are the temperatures of various thruster components as a function of on axis solar illumination of 0, 1, and 2 suns for a 2 amp beam current. As shown in the figure, with the 360° shield at 250° C and 2 suns illumination, the cathode tee coupling increased in temperature to 289° C. This increase in feed line temperature (the tee coupling is attached to a structural support-back of the manifold member)⁶ caused a loss of control of the cathode vaporizer and even at

zero power to the vaporizer the vaporizer temperature increased to 287° C from its nominal 282° C. There was no loss of control of the main vaporizer for operating at 311° C, it was not adversely effected by the lower 285° C temperature of the main tee coupling. A lower value of conductance of the cathode vaporizer plug, allowing a higher operating temperature or thermally isolating the feed line-tee coupling from the manifold-support structure would alleviate this problem. (A thermocouple placed on the support structure rendered the same temperature as the tee coupling.) Because of this cathode vaporizer problem, new vaporizer plugs are being made that will operate for a 2 amp beam at greater than 300° C.

Shown in Figure 20 are the corresponding vaporizer power levels for the thruster-temperature levels shown in the previous Figure 19, for a 2 amp beam current. An increase in solar illumination to 2 suns, although reducing the power requirement for the main vaporizer and neutralizer vaporizer, leaves adequate margin for control of these two vaporizers. Also shown on Figure 20 are the 360° azimuthal shield temperatures that correspond to a given thruster operating configuration. At one sun illumination and a shield temperature of 230° C there is control of the cathode vaporizer, the power being 0.9 watts. At two suns, power requirements are shown for three different background 360° shield temperatures. As the shield temperature increases from 180° C to eventually 250° C, control of the cathode vaporizer is lost. (At 2 suns, $J_B = 2A$, and 0 power applied to the 360° shield, the shield temperature is 150° C. With zero sun and the same conditions the shield temperature is 100° C.) At lower beam currents and 2 suns, because of the lower thruster operating temperatures, no such problems were encountered.

For 0, 1, and 2 suns illumination and shield temperatures of up to 250° C for thermal configuration III there were no changes in beam profile as measured by the moly button probe. This means no change in thrust vector. No change in preveance occurred for thermal configuration 3, at 2 suns and a beam current of 2 amps, for an accelerator grid temperature as high as 272° C. The extreme thermal constraints imposed on the thruster by thermal configuration 3 and 2 suns illumination caused no high voltage breakdowns or changes in thruster performance level (i.e., utilization). There was also no evidence of thermal warping of the grids.

Thermal Configuration IV

Thermal configuration IV was similar to thermal configuration III, except a 270° azimuthal shield was used instead of a 360° shield to simulate asymmetric thermal loading of the thruster. This configuration allowed the top of the thruster a 25 percent azimuthal view factor to LN₂ walls, a realistic thruster thermal configuration. The thruster was run at quarter, half, and full beam power at 0, 1, and 2 suns illumination. Shown in Figure 21 are the temperature levels for various thruster components, at $J_B = 2A$, $J_E = 10A$, and $\Delta V_1 = 37V$ for 0, 1, and 2 suns. Because of the 270° shield is in the lower quadrants there was a very large azimuthal thermal gradient on the ground screen, the engine body, and anode. The top of the ground screen is 100° C cooler than the ground screen at the bottom for all sun conditions. This large azimuthal thermal gradient caused no notice-

able thruster operation problems. Because of the azimuthal view factor, the rear cover for this configuration runs cooler than for thermal configuration III, for all conditions tested. The cathode feed line tee coupling was at 265° C and the 270° shield was at 240° C at full beam power and 2 suns illumination. Thus, in this case, (as shown in Fig. 22) there was no loss of control of the cathode vaporizer, due to excess thermal input from the feed line. The SS/Al Mylar rear shield temperature is also plotted in Figure 21 and shows, a sink temperature for the rear of the thruster of 102° C to 122° C. These high rear shield temperatures to which the rear of the thruster had to radiate did not effect thruster operation.

Shown in Figure 22 are the configuration IV vaporizer power values for 3 different thruster power settings (1/2, 1, and 2 amp beam currents) as a function of sun illumination. As shown in the figure the neutralizer vaporizer power setting at $J_B = 1$ and 2A was nearly insensitive to solar illumination. At a 1/2 amp beam current the neutralizer vaporizer power setting decreases with solar illumination, but at all sun conditions it has a higher power setting than for $J_B = 1$ or 2 amps. Thus, in thermal configuration 4 there is plenty of margin for control of the neutralizer. Likewise, the main vaporizer has plenty of control margin, for even at $J_B = 1/2 A$ and 2 suns illumination, the lowest power setting is 4 watts. For the cathode, at $J_B = 2A$ and 2 suns illumination, the cathode vaporizer was controllable at 0.9 watts. Thus, a 30 cm EM thruster in thermal configuration 4 has no problems w.r.t. control of the vaporizers, even at a 270° shield temperature of 240° C and 2 suns illumination.

For the conditions tested in thermal configuration IV, there were no changes in beam profile or preveance. Again, no change in thruster vector. Thus assymmetric thermal loading did not change thruster performance level or cause grid warping or high voltage breakdowns.

VI. Concluding Remarks

The Engineering Model thruster was cold soaked at background temperatures of -196° C. No structural changes resulted during or after cold storage and the thruster was restarted without any noticeable problems. It was shown that if the Hg feed lines are thawed up to the rear cover it was possible to restart the thruster from thruster temperatures as low as -81° C to full beam power in 34 minutes with a minimum of breakdowns.

The thruster operated satisfactorily after eclipse simulations that varied in length from a little as 17 minutes to as long as 72 minutes. It was possible to return to full beam power, on laboratory power supplies, in as little as 15 minutes with little or no breakdowns. However, the duration of the eclipse can affect the restart sequencing of the thruster.

The thruster was run through extensive thermal testing under a variety of multiple thruster, plus sun illumination. Thruster control characteristics were evaluated over a range of thruster power settings, from 1/4 to full beam power. With the 700 series EM thruster it was possible to thermally isolate the thruster from the rearward hemisphere and other thrusters at 1 sun solar illumina-

tion. At 2 suns solar illumination rearward hemisphere isolation was possible, but not total thruster isolation. At 2 suns, in the total isolation case, control was lost for the cathode vaporizer, but not for the main or neutralizer vaporizers. At all multiple thruster and 2 sun conditions run there was no changes in either thruster performance level or in the thrust magnitude or directions.

The thruster maintained structural integrity over the range of thermal environments. There were no indications of impact on thruster lifetime.

Enough data was generated to thermally characterize the thruster and provide data for a future theoretical thermal model. This information can be used to characterize thruster performance in proposed spacecraft-mission configurations.

References

1. Wen, L. C. and Womak, J. R., "Thruster Array Thermal Control," AIAA Paper 73-1117, Lake Tahoe, Nev., 1973.
2. Horio, S. P. and Gutter, C. H., "SEP Stage for Earth Orbital Missions---Solar Electric Propulsion Stage for Shuttle/Tug Payload Increase," AIAA Paper 73-1123, Lake Tahoe, Nev., 1973.
3. Ruttner, L. E., "Thermal Control of the Solar Electric Propulsion Stage," AIAA Paper 73-1118, Lake Tahoe, Nev., 1973.
4. Mirtich, M. J., "The Effects of Exposure to LN₂ Temperatures and 2.5 Suns Solar Radiation in 30-cm Ion Thruster Performance," AIAA Paper 75-343, New Orleans, La., 1975.
5. Poeschel, R. L., King, H. J., and Schnelker, D. D. E., "An Engineering Model 30-cm Thruster," AIAA Paper 73-1084, Lake Tahoe, Nev., 1973.
6. Collect, C. R., and Bechtel, R. T., "15 000 Hour Endurance Test of an Advanced 30-cm Ion Thruster," Proposed AIAA Paper 76-1023, Key Biscayne, Fla., 1976.
7. Jack, J. R., and Spiez, E. W., "Environmental Simulation from 0.01 to 100 Solar Constants," TM X-68048, 1972, NASA.
8. Bechtel, R. L., "Central Logic for a 30-cm Diameter Ion Thruster," AIAA Paper 75-378, New Orleans, La., 1975.
9. Robson, R., "Compensated Control Scope for a 30-cm Ion Thruster," Proposed AIAA Paper 76-994, Key Biscayne, Fla., 1976.
10. Bechtel, R. L., Private Communication, 1974.
11. NAS 3-17803, "Fabrication and Verification Testing of EMT 30-cm Diameter Ion Thruster."

ORIGINAL PAGE IS
OF POOR QUALITY

TABLE I. - THRUSTER-ENVIRONMENT CONDITIONS FOR SOLAR-THRUSTER SIMULATION TESTS

Test	Thruster conditions					Thermal environment				
	Thruster conditions		Vaporizer power, W			Thermal configuration	Number of suns	Azimuthal shield		Rear shield temperature, °C
	J _B , A	J _E , A	ΔV _T , V	Main	Cathode			Neutralizer	Type, deg	
1	2	10	37	6.4	4.3	4.1	1	---	---	34
2	2	10	37	5.0	2.1	3.3	1	---	---	40
3	1	6	37	5.3	4.7	4.1	1	---	---	35
4	1	6	37	5.3	3.8	3.8	1	---	---	32
5	1/2	3	37	5.6	7.2	5.1	1	---	---	52
6	1/2	3	37	5.6	6.0	4.3	1	---	---	39
7	2	10	37	5.6	2.4	4.1	2	---	---	36
8	2	10	37	4.8	1.2	3.5	2	1	360	58
9	2	10	37	4.6	.5	3.0	2	2	360	51
10	1	6	37	8.0	4.1	5.0	2	---	---	23
11	1	6	37	5.0	2.2	5.4	2	2	360	36
12	1/2	3	37	6.4	6.6	5.1	2	---	---	22
13	1/2	3	37	5.6	5.1	4.1	2	2	360	26
14	1/2	3	37	5.6	6.3	3.2	3	---	---	54
15	1/2	3	37	4.3	5.8	3.2	3	1.1	360	73
16	1	6	37	5.6	3.2	2.5	3	---	---	61
17	1	6	37	4.8	3.0	1.9	3	1.1	360	95
18	2	10	37	5.0	1.7	3.0	3	---	---	108
19	2	10	37	4.7	.9	2.7	3	1.1	360	116
20	2	10	37	4.4	0	2.5	3	2	360	119
21	1/2	3	37	5.6	6.6	5.2	4	---	---	42
22	1/2	3	37	4.7	6.6	4.7	4	1	270	47
23	1	6	37	6.4	4.3	4.2	4	---	---	56
24	1	6	37	5.6	3.7	4.0	4	1	270	79
25	2	10	37	5.6	1.9	3.2	4	---	---	102
26	2	10	37	5.0	1.3	3.2	4	1	270	104
27	2	10	37	5.0	.9	3.1	4	2	270	122
28	2	10.6	35	5.6	1.9	3.2	4	270	210	105
29	2	10.6	35	4.5	.9	3.2	4	270	237	120

PRECEDING PAGE BLANK NOT FILMED

TABLE II. - THRUSTER TEMPERATURE LEVELS IN °C FOR CONDITIONS DEFINED IN TABLE I

Thermocouple location	Test number																
	1	2	3	4	5	6	7	8	9	10	11	12	13	14	15	16	17
Main tee coupling, 2	199	226	163	191	113	155	245	261	275	203	240	155	196	165	194	219	240
Main vaporizer, 3	314	314	292	292	268	271	311	311	312	295	296	270	271	265	266	286	286
Main vaporizer base, 4	248	278	207	242	157	205	277	298	308	234	273	183	230	189	222	243	264
Mainfold, 5	240	276	194	236	136	196	274	295	311	225	271	168	226	177	218	239	265
Cathode, I.V. base, 6	246	277	209	243	168	215	277	295	309	236	275	193	239	201	234	248	270
Manifold, near cathode tee, 7	239	275	193	234	134	196	275	293	311	226	273	168	226	178	216	239	263
Cathode vaporizer, 8	280	280	281	282	300	301	282	284	282	284	285	299	300	303	304	289	290
Cathode flange, 9	404	412	365	376	322	342	414	420	421	365	380	327	344	335	351	396	403
Inner magnetic retainer, 10	372	397	311	339	239	283	393	402	415	325	357	254	294	266	295	351	368
Cathode tee coupling, 11	206	230	173	195	133	165	252	266	280	211	246	166	205	176	203	227	246
Engine body																	
Center, 90°, 14	166	193	129	158	75	121	241	253	274	198	237	140	189	152	182	210	231
Front, 90°, 15	228	260	177	213	105	163	280	299	312	224	266	155	212	164	198	236	259
Back, 180°, 16	175	204	135	166	81	129	241	253	276	195	236	138	189	150	182	206	228
Center, 270°, 18	166	194	129	158	76	121	247	258	281	205	244	144	196	155	186	212	233
Front, 270°, 19	220	254	173	209	105	161	288	307	323	233	277	164	222	172	209	240	264
Top downstream ring, 13	243	275	192	230	123	183	285	302	319	232	276	166	226	174	211	240	265
Bottom downstream ring, 17	238	267	184	221	114	173	279	297	312	225	268	157	216	164	202	234	259
Anode, back, 270°, 22	244	277	193	234	128	190	277	296	313	225	271	160	221	169	205	234	260
Anode, front, 270°, 23	401	425	337	363	245	281	451	460	468	368	396	275	314	283	306	373	386
Accelerator, 270°, 21	154	222	118	198	64	177	197	239	267	160	239	107	209	105	186	161	217
Neutralizer tip, 28	650	653	607	618	599	599	598	600	603	586	594	579	586	595	605	611	618
Neutralizer vaporizer, 26	277	277	277	277	280	282	282	282	282	297	297	291	296	282	282	282	282
Ground screen, top, 24	79	98	67	80	28	58	214	230	248	183	218	131	175	144	172	191	211
Ground screen, 270°, 21	47	68	30	45	-6	24	212	229	247	181	218	123	173	139	166	188	205
Rear, cover, top, 29	106	126	86	102	47	78	187	198	216	157	189	112	152	130	157	174	192
Rear, cover, in, 27	101	120	81	96	43	73	170	183	195	141	170	101	137	122	148	163	180

TABLE II. - Concluded.

Thermocouple location	Test number											
	18	19	20	21	22	23	24	25	26	27	28	29
2	256	272	284	145	148	188	206	236	249	264	236	265
3	308	308	308	270	269	295	295	315	315	315	316	316
4	283	301	314	178	201	224	244	273	286	302	273	303
5	283	304	319	162	192	216	239	269	285	304	269	305
6	284	302	316	186	208	223	243	268	268	298	266	298
7	282	302	318	158	186	210	234	263	280	299	263	298
8	282	282	287	301	302	284	284	280	280	280	281	281
9	426	430	429	326	331	368	374	406	410	421	410	421
10	405	418	423	250	267	320	335	384	394	410	382	409
11	263	277	289	157	171	194	209	238	250	264	237	265
Engine body												
14	245	260	277	124	148	172	192	226	240	256	226	256
15	283	298	316	143	172	205	227	268	284	300	267	299
16	245	261	280	132	157	181	202	237	253	270	239	271
18	248	263	282	131	155	178	198	233	249	265	233	265
19	289	306	324	149	176	207	230	270	287	304	269	302
13	290	307	323	145	173	203	224	261	278	293	261	292
17	283	300	316	152	180	213	235	274	290	305	274	305
22	283	301	319	155	183	211	234	269	284	303	270	304
23	455	463	472	261	281	344	360	423	438	447	419	438
21	198	238	272	100	152	146	184	192	225	257	197	261
28	659	657	600	593	596	596	610	643	644	648	643	646
26	280	280	280	283	283	276	276	280	280	280	280	280
24	213	228	245	47	62	74	84	102	111	123	100	121
21	208	220	243	111	132	131	169	204	216	230	203	232
29	202	124	229	92	108	115	140	163	174	186	163	187
27	190	202	215	92	108	115	141	166	175	187	173	198

ORIGINAL PAGE IS
OF POOR QUALITY

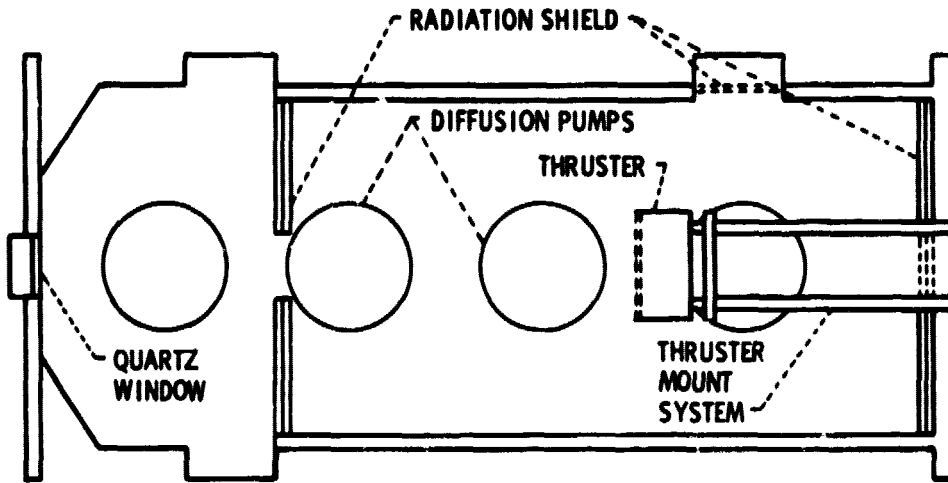


Figure 1. - Vacuum tank and thruster position in tank.

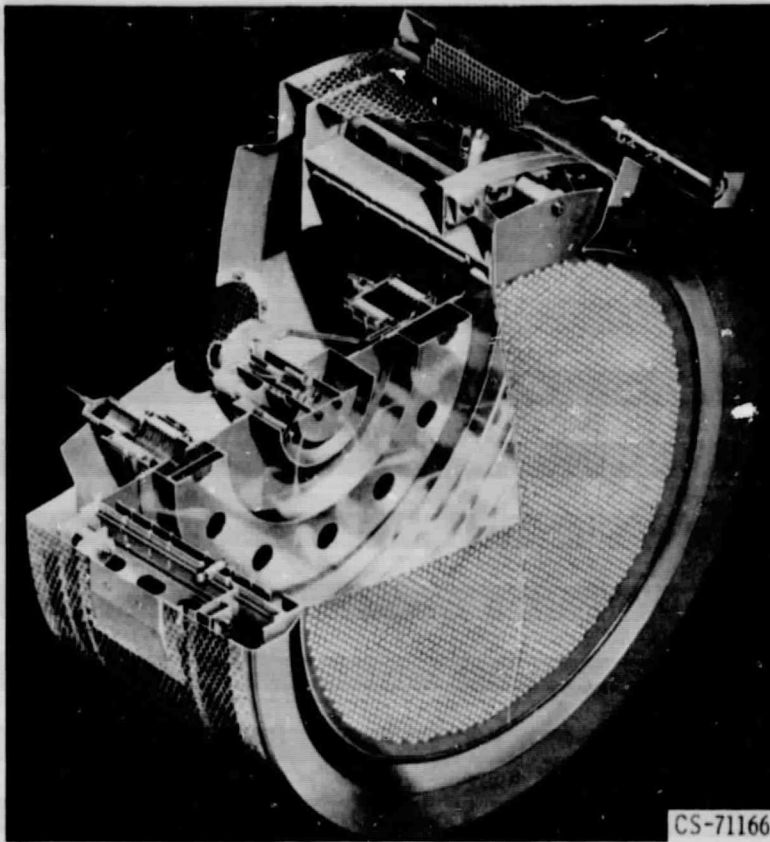


Figure 2. - Hughes 700 series 30 cm thruster.

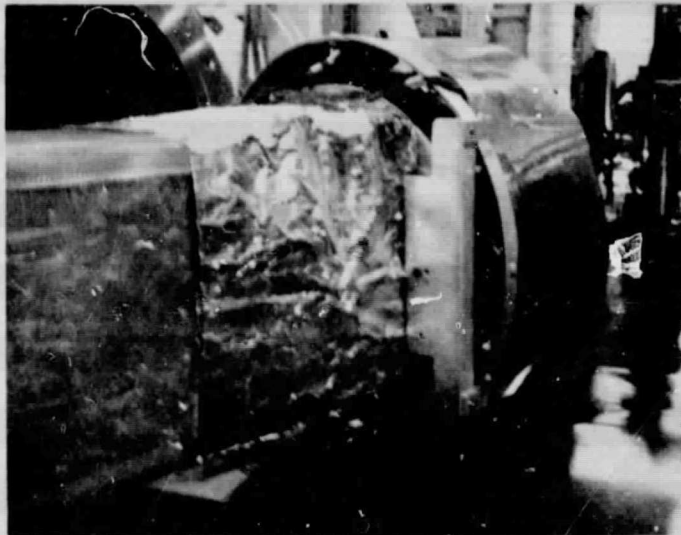


Figure 3. - Back view of thruster and mount system.

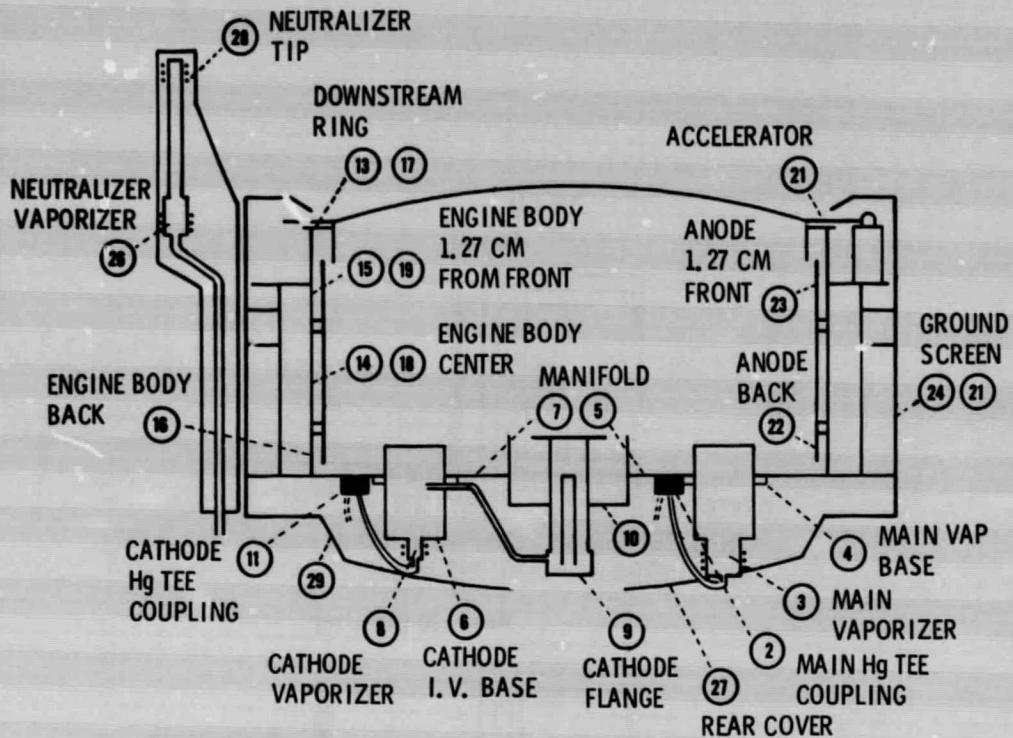


Figure 4. - Thermocouple locations on EM thruster.

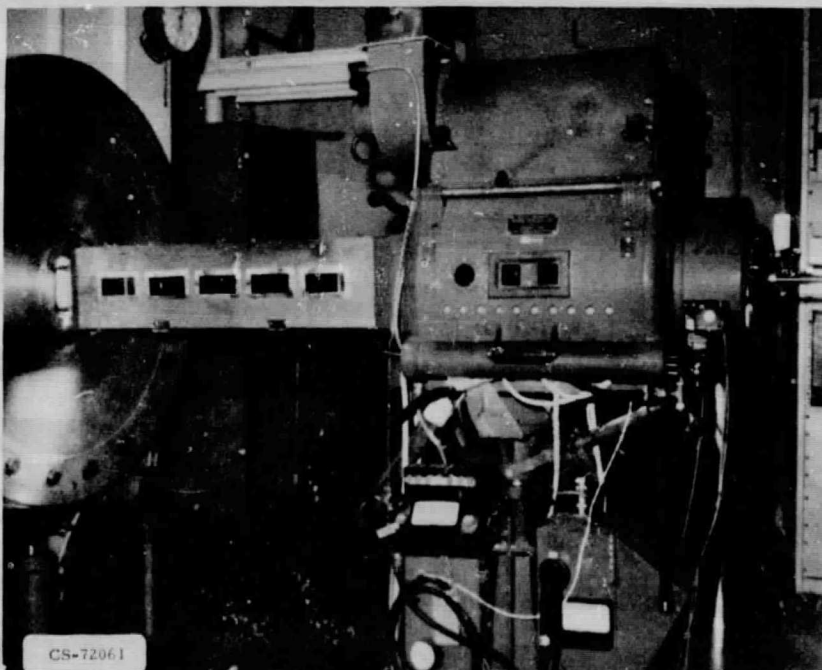


Figure 5. - 40 kW Carbon arc solar simulator.

ORIGINAL PAGE IS
OF POOR QUALITY

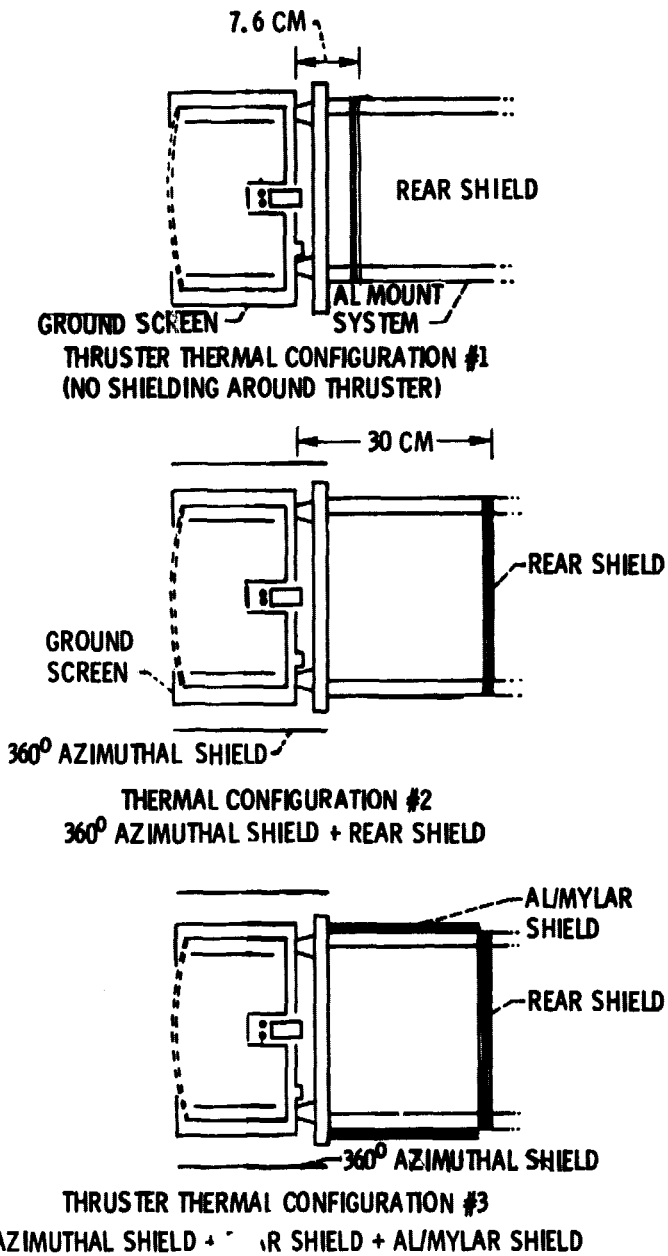


Figure 6. - Thruster thermal configurations used in the thermal tests.

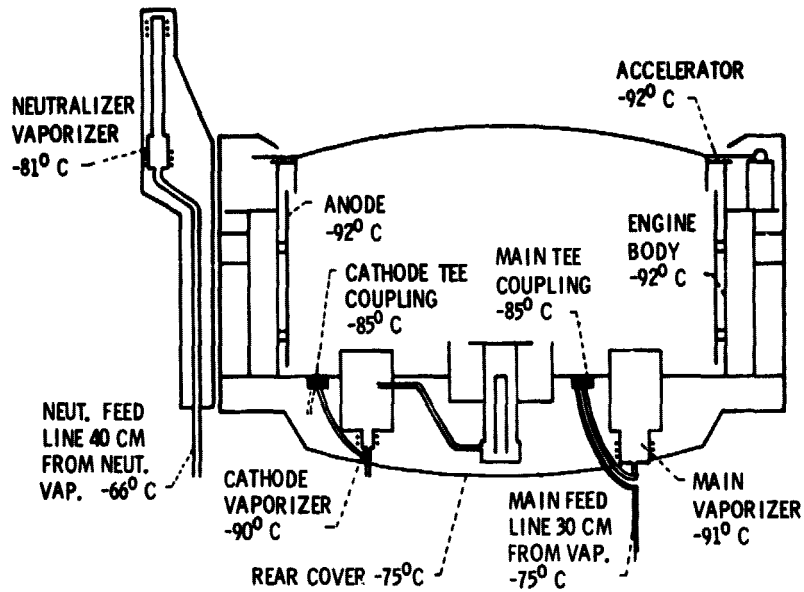


Figure 7. - Cold storage temperatures on thruster for thermal configuration 1.

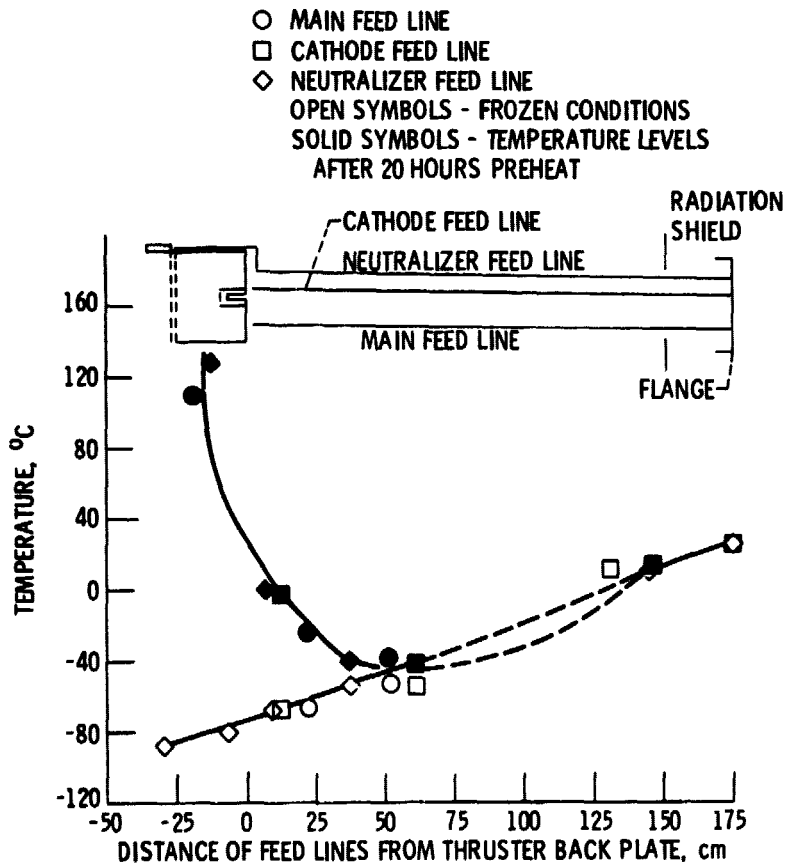


Figure 8. - Feedline temperature levels at various distances from the thruster backplate.

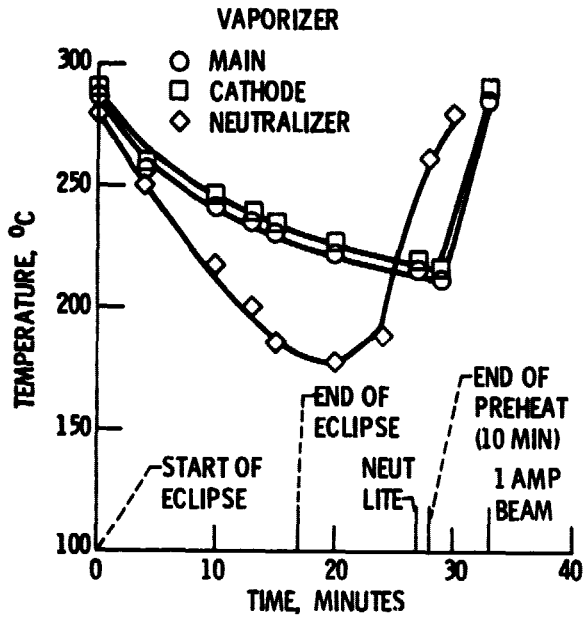
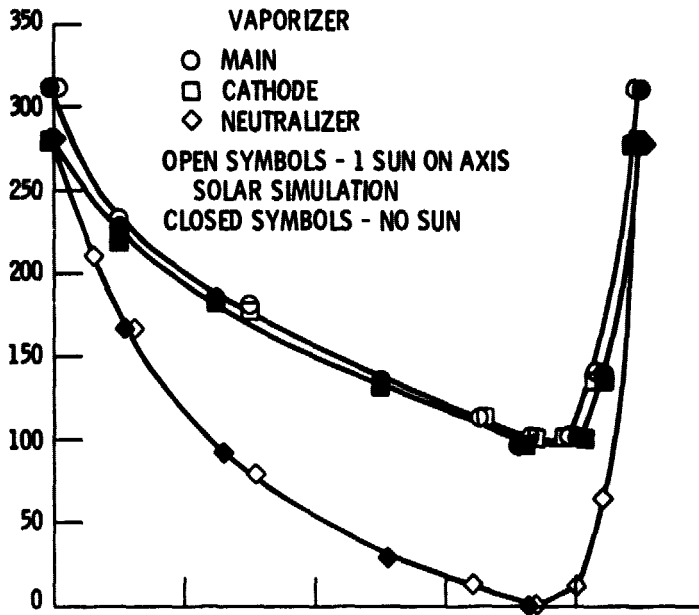
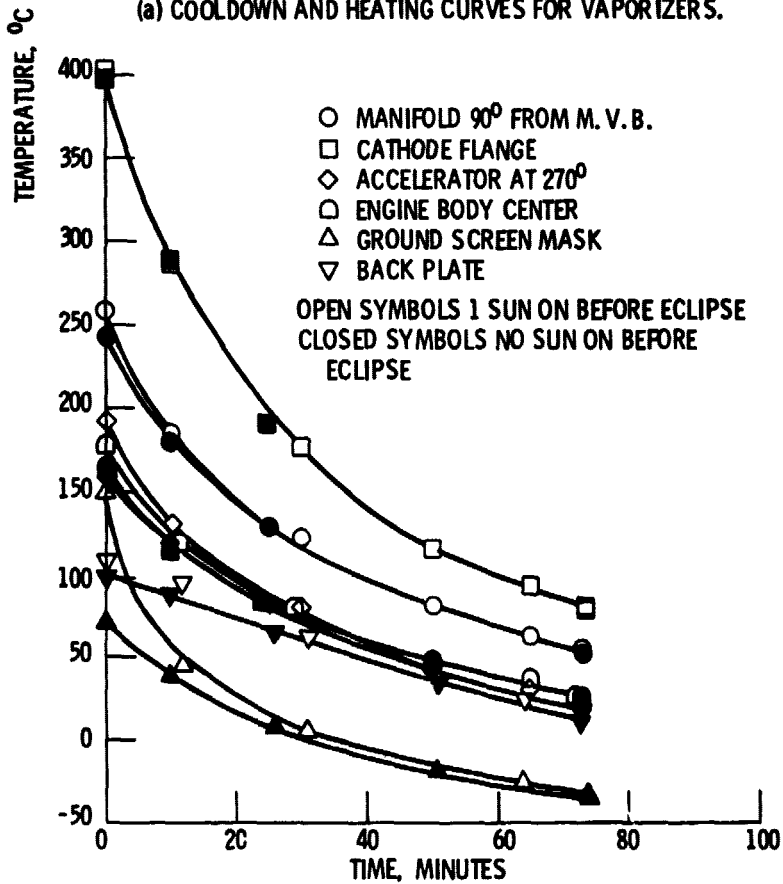


Figure 9. - Cooling and heating curves for a 17 minute eclipse. Thruster back to 1 amp beam in 16 minutes.



(a) COOLDOWN AND HEATING CURVES FOR VAPORIZERS.



(b) COOLDOWN CURVES DURING 72 MINUTE ECLIPSE FOR VARIOUS THRUSTER COMPONENTS.

Figure 10. - Cooldown curves during eclipse for thruster facing and not facing 1 sun before 72 minute eclipse.

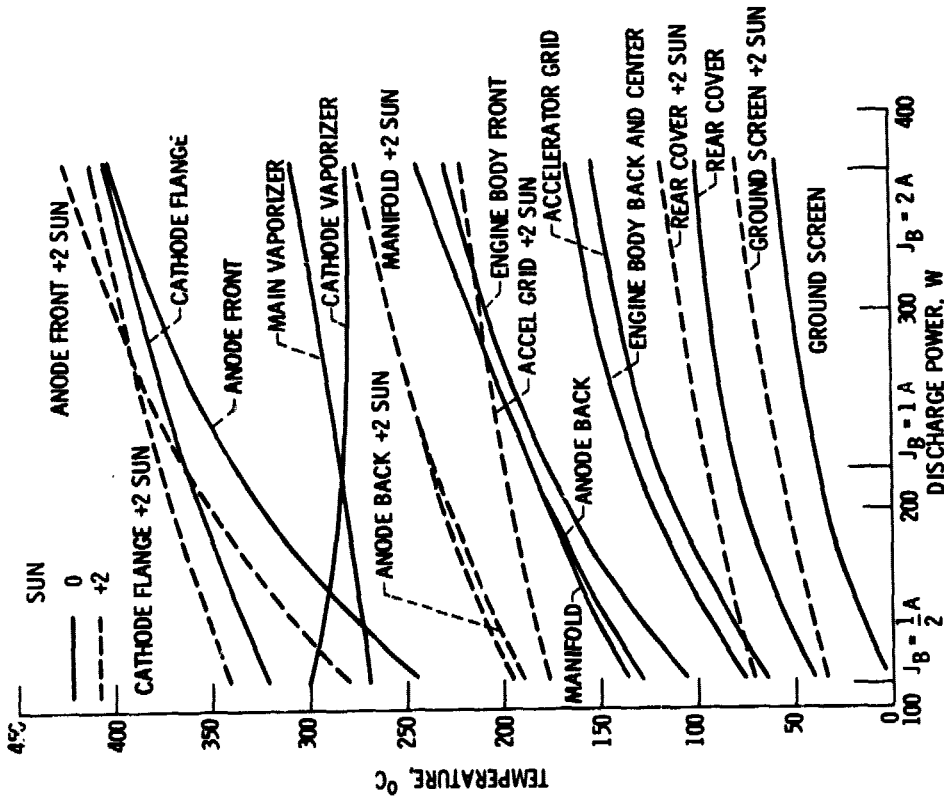


Figure 11. - Temperature levels of various thruster components as a function of discharge power; thermal configuration I, single operating thruster.

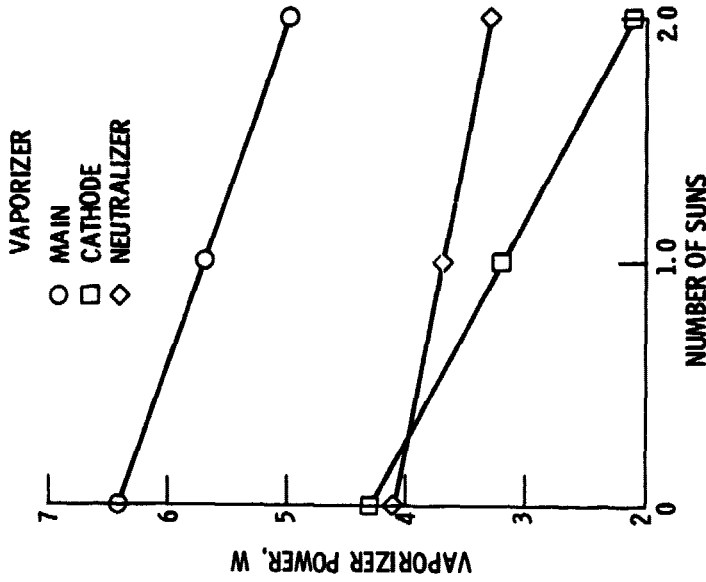


Figure 12. - Thermal configuration I; $J_B = 2 \text{ A}$, $\Delta V_1 = 37 \text{ V}$, $J_C = 10 \text{ A}$.

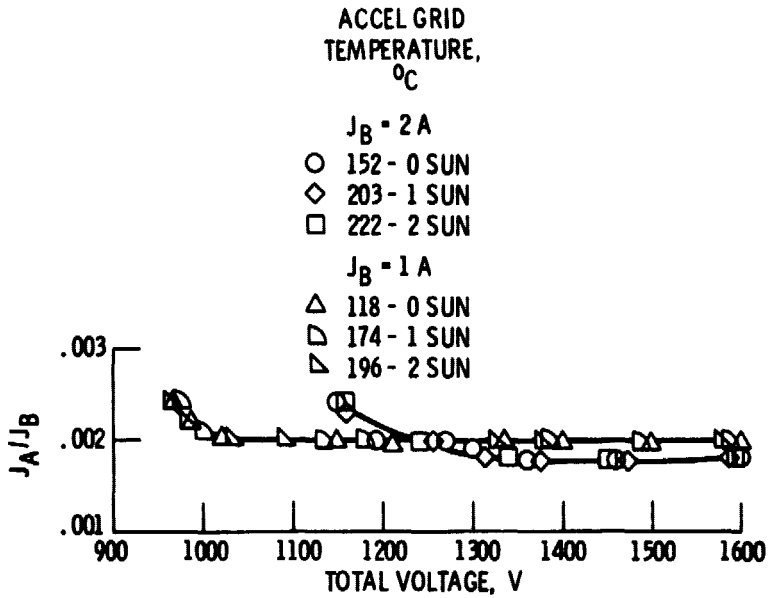


Figure 13. - Plot of J_A/J_B versus total voltage for thermal configuration I.

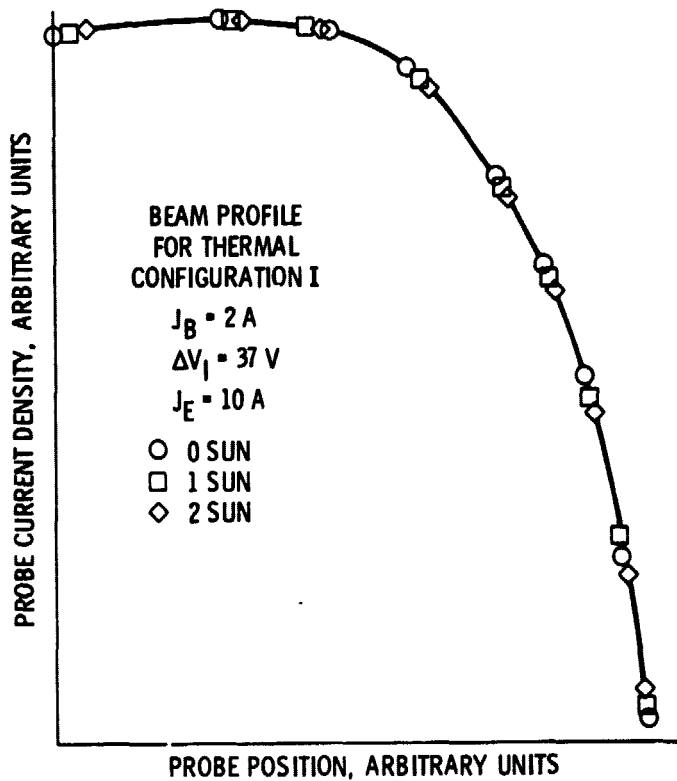


Figure 14. - Beam profile for various sun levels at $J_B = 2 \text{ A}$.

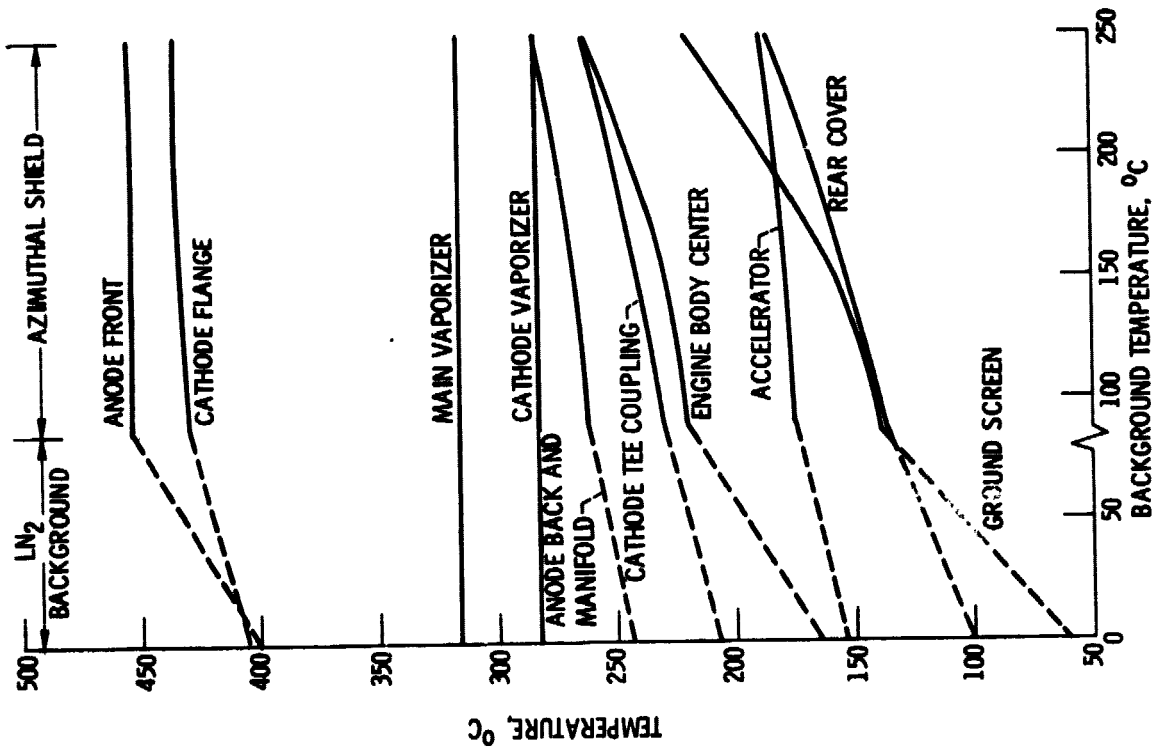


Figure 16. - Effect of azimuthal temperature levels on thruster temperature levels for full beam power, J_B = 2 A and 0 sun.

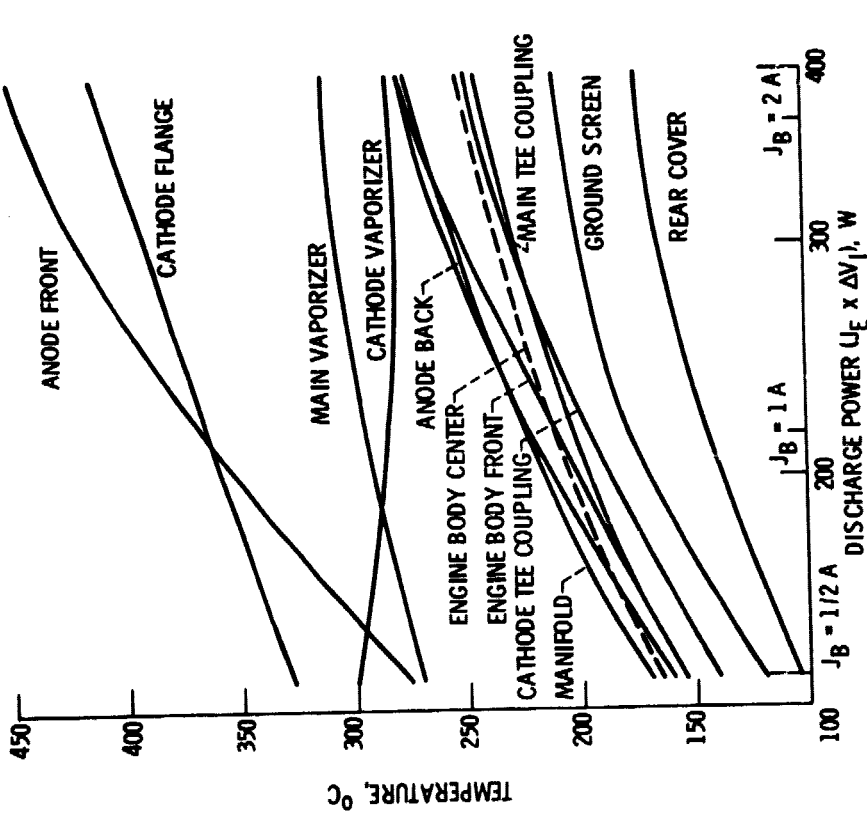


Figure 15. - Temperature levels of various thruster components as a function of discharge power for thermal configuration II and no sun.

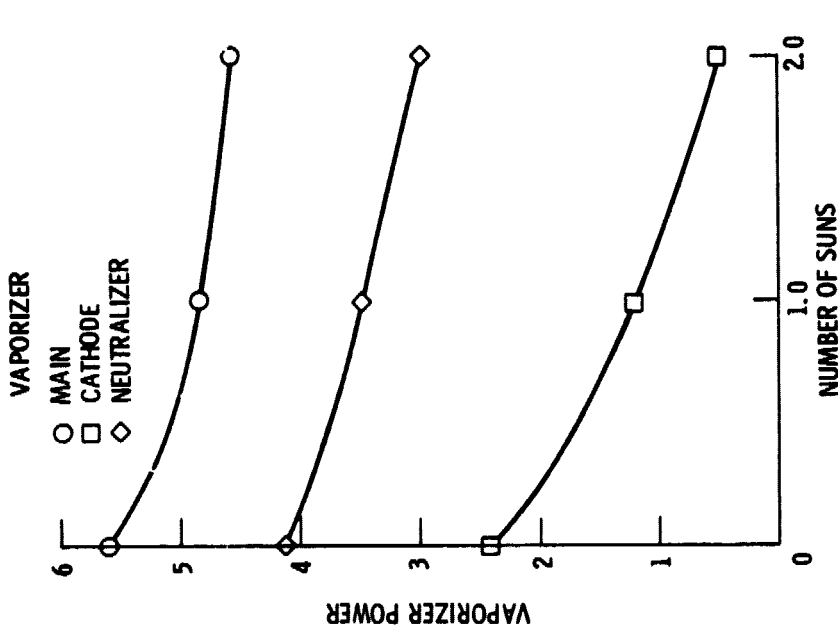


Figure 17. - Vaporizer power settings as a function of solar illumination for full beam power; thermal configuration II, $J_B = 2 \text{ A}$, $\Delta V_I = 37 \text{ V}$, $J_E = 10 \text{ A}$.

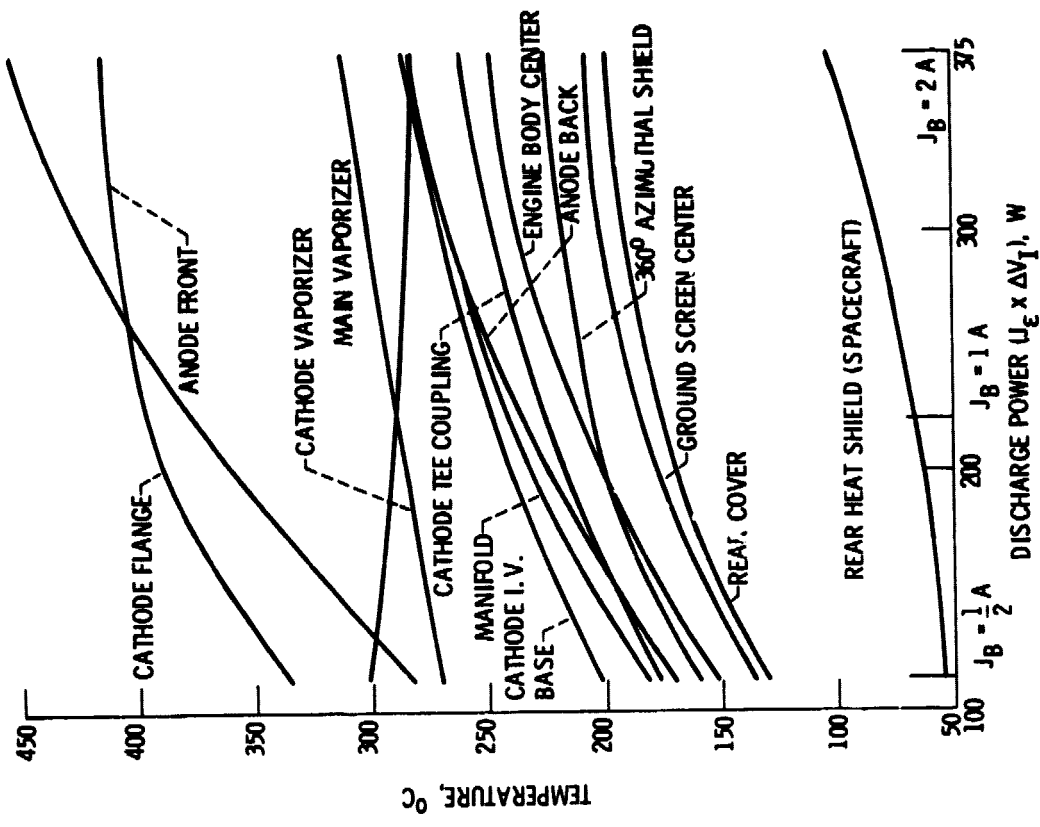


Figure 18. - Temperature levels of various thruster components as a function of discharge power for thermal configuration III and no sun.

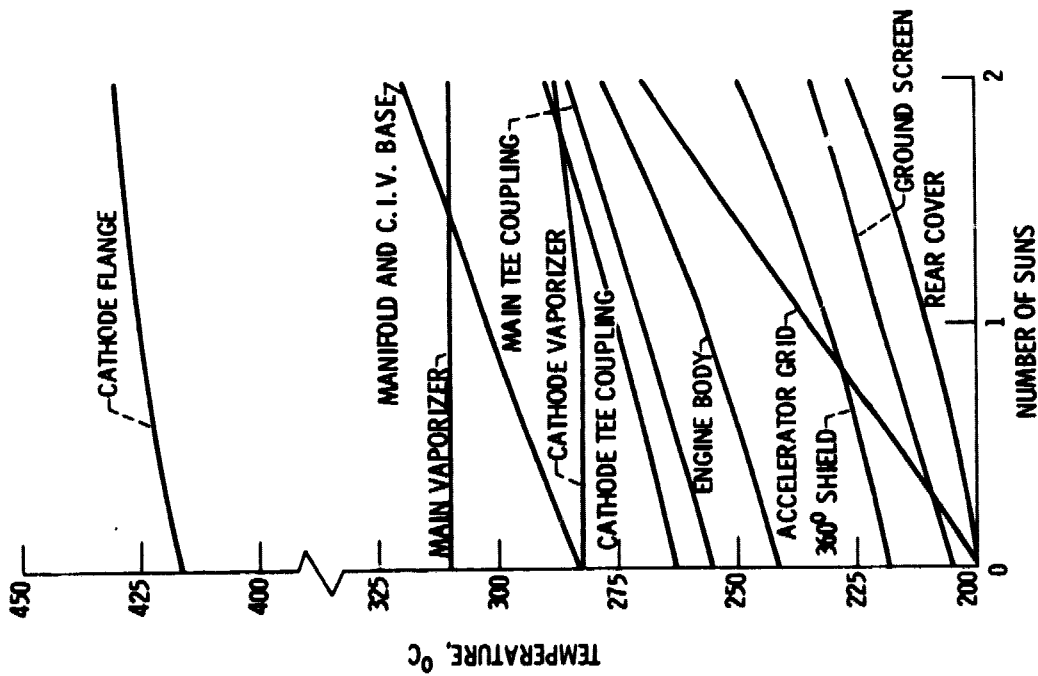


Figure 19. - Temperature levels of thruster components as a function of solar illumination for thermal configuration III and $J_B = 2 \text{ A}$.

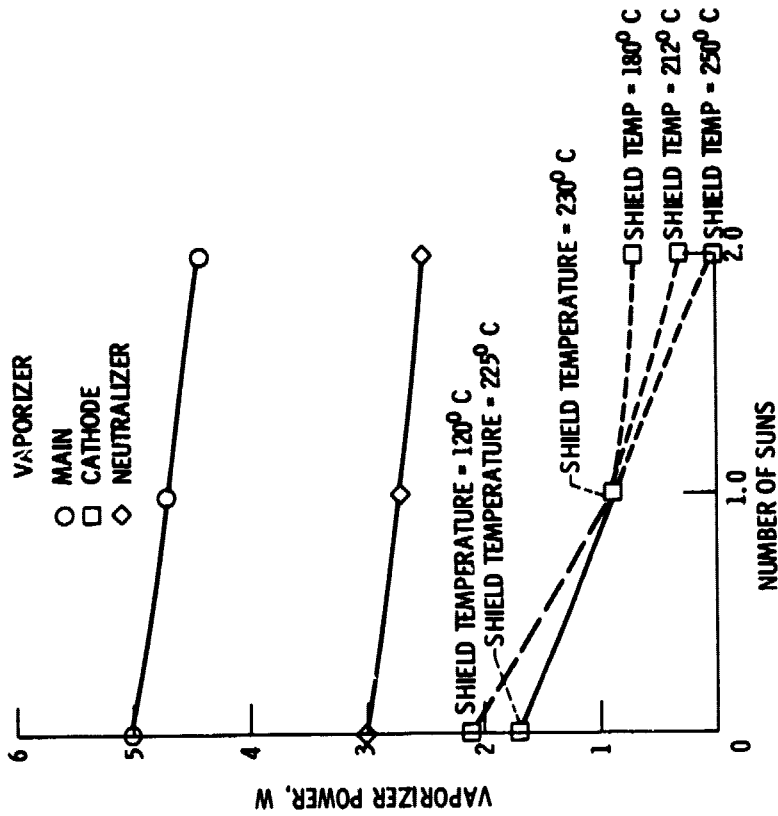


Figure 20. - Vaporizer power settings as a function of solar illumination for full beam power and thermal configuration III; $J_B = 2 \text{ A}$. $\Delta V_I = 37 \text{ V}$, $J_C = 10 \text{ A}$.

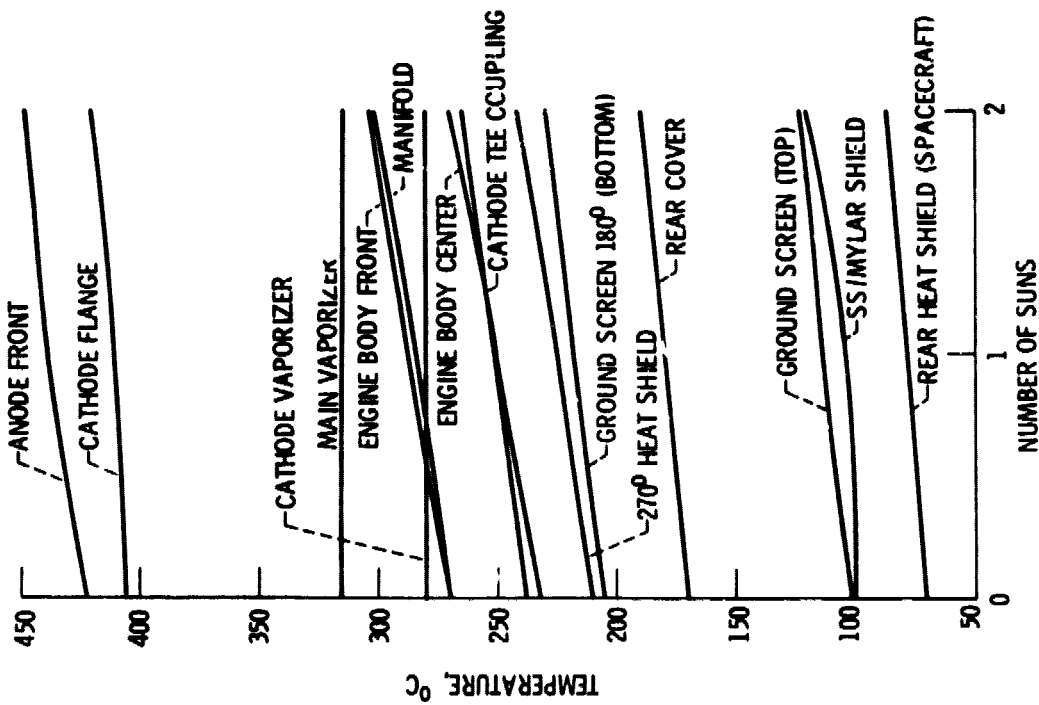


Figure 21. - Temperature level of various thruster components for thermal configuration IV and $J_B = 2 \text{ A}$ as a function of solar illumination; thermal configuration IV, 270° shield, $J_B = 2 \text{ A}$, $\Delta V_I = 37 \text{ V}$, $i_e = 10 \text{ A}$.

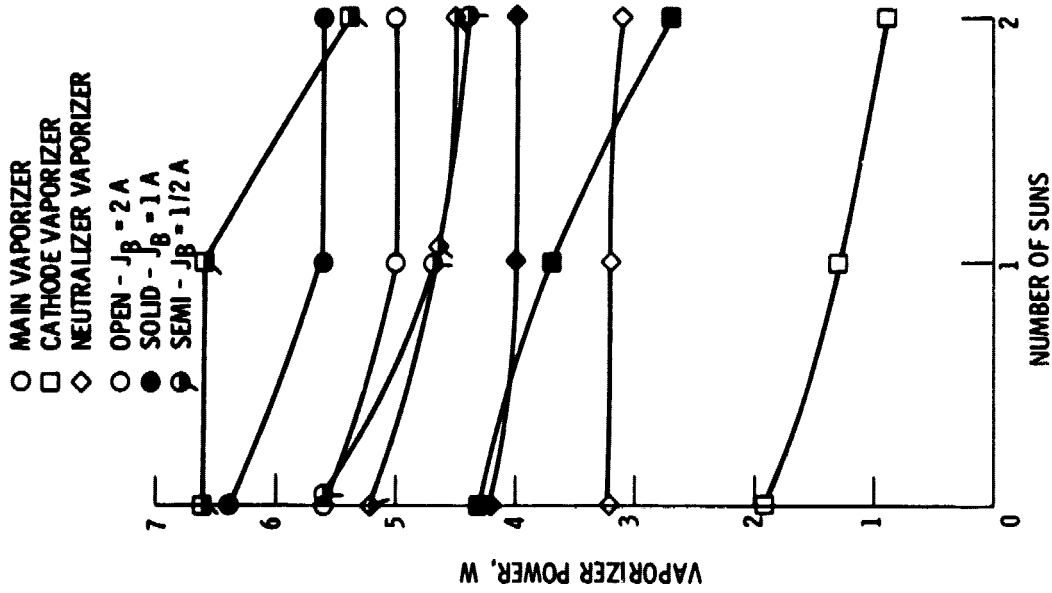


Figure 22. - Vaporizer power setting for various beam currents as a function of solar illumination for thermal configuration IV.